

# Practical Predictive Control Strategy for Efficient Harnessing of Marine Energy

Mohamed Jama

*Department of Electrical, Computer and Biomedical Engineering  
Abu Dhabi University  
Abu Dhabi, United Arab Emirates  
mohamed.jama@adu.ac.ae*

Abdelrahman Omer Idris

*Network Operation Department  
Al Ain Distribution Company (AADC)  
Al Ain, United Arab Emirates  
abdelrahman-po@aad.ac.ae*

**Abstract**—The control challenge in marine energy remains an ongoing research query due to the complexities involved in developing effective and economically viable control strategies. To address these challenges, this study proposes a predictive control strategy based on finite control set model approach for point absorber wave energy harvesters (WEHs). The developed control strategy deploys a comprehensive nonlinear system model specifically designed for vertically oscillating WEHs. By formulating the predictive control in the finite set control framework, the control objective is achieved without the need for a predefined control command trajectory. Instead, the strategy searches for optimal control laws, in the form of power converter switching functions, to maximize the converted electrical energy of the WEH. Simulation is conducted to evaluate the efficacy of the suggested controller. The results clearly demonstrate that the suggested approach outperforms its benchmark reference-based counterpart in both the conversion efficiency and also in the required PTO control effort.

**Index Terms**—Wave energy, predictive control, permanent magnet linear generator, nonlinear model

## I. INTRODUCTION

When compared to other prominent green energy sources, marine energy remains significantly underutilized as a renewable energy source. Despite its immense potential and significant power density (i.e., 10 times of that of wind energy), marine energy is yet to be extensively harnessed [1]. The feasibility of wave energy harvesters (WEHs) is predominantly influenced by elements like the accessible wave energy potential, the selected WEH design, the efficiency of the power extraction system, and the governing control approach. These elements play a crucial role in determining the feasibility and success of wave energy utilization [2]. The control problem in wave energy harvesters (WEHs) is characterized by high complexity due to the presence of multiple interacting systems, each with its own operating principles and physical constraints [3].

Throughout the years, various categories of control strategies have been put forward in the literature. The fundamental idea underlying most of these strategies revolves around the concept of achieving optimum (maximum) power transfer, such as resistive loading (RL) and approximate complex conjugate (ACC) [4]. The application of model predictive control (MPC) strategies poses its own set of challenges when it comes to addressing the control problem in WEHs [4].

Function-based MPC is discussed in [5]. In addition, model-free control techniques have been extensively investigated to control various types of WEHs, examples of such controller are reported in [6], [7] and deep learning and machine learning based controllers in [8]. Power point tracking algorithms have been investigated in numerous studies, such as [9], [10].

In this study, a novel reference-less (RL) predictive control strategy is introduced for the effective control of point absorber WEH. Unlike servo-control strategies, this control approach does not rely on determining an online reference trajectory. Instead, it is based on solving an online constrained optimization problem using a search algorithm to maximize the energy captured by the PTO system. The proposed technique enables the determination of an optimal set of switching states, selected from a possible eight options, for controlling the current in the stator circuit of the machine-side converter. By leveraging the nonlinear nature of finite control set based predictive control, a holistic wave-to-wire mathematical model of the WEH can be effectively utilized within a single predictive control framework. This paper is organized as follows: Section II discussed the WEH full model. Section III outlines the proposed control strategy. Section IV briefly describes a traditional reference-based control strategy used as benchmark to evaluate the proposed control strategy. Results are discussed in Section V. Finally, conclusions were drawn in Section VI.

## II. WEH MODEL

In this work, the WEH under investigation utilizes a semi-spherical buoy that oscillates against a fixed platform, as depicted in Figure 1. The vertical motion of the buoy, known as heave motion, directly powers a power take-off (PTO) system. In this section, a comprehensive nonlinear dynamic model is developed to describe the behavior and performance of the WEH configuration being studied, encompassing the entire wave-to-wire model.

The point absorber WEH can be modeled as [2]

$$\begin{aligned} \theta_e(t) - \theta_r(t) - \theta_b(t) - \theta_s(t) - \theta_d(t) \\ - \theta_f(t) - \theta_m(t) = ma(t), \end{aligned} \quad (1)$$

where  $\theta_e(t)$ ,  $\theta_r(t)$ ,  $\theta_b(t)$ ,  $\theta_s(t)$ ,  $\theta_d(t)$ ,  $\theta_f(t)$ , and  $\theta_m(t)$  are the excitation, radiation, hydrostatic, PTO restoring, viscous drag, friction, and PMLG forces, respectively. The symbols  $m$  and

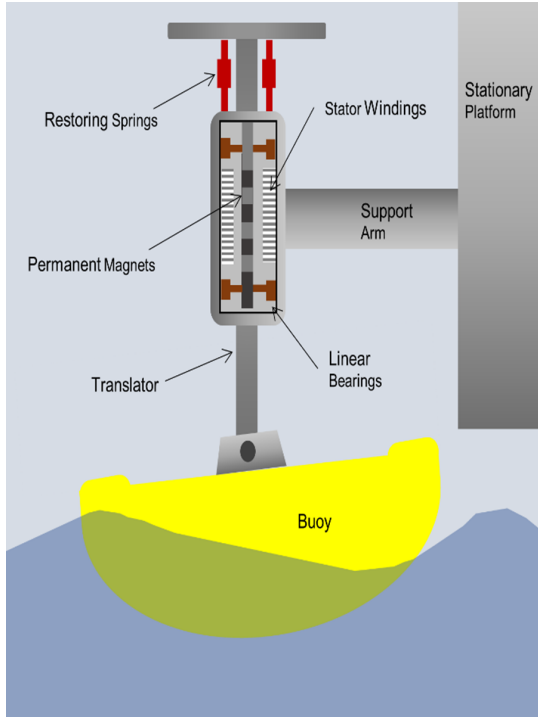


Fig. 1. WEH overview.

$a(t)$  represent the mass and vertical acceleration of the buoy, respectively. The developed modeled can be further elaborated into

$$\begin{aligned}
 a(t) = & \frac{1}{m + m_{inf}} \left[ \theta_e(t) - \mathbf{C}_r \boldsymbol{\sigma}(t) - \underbrace{S_s x(t)}_{\theta_s(t)} \right. \\
 & - \underbrace{\pi \rho g r_b^2 \left( 1 - \frac{|x(t)|x(t)}{3r_b^2} \right) x(t)}_{\theta_b(t)} \\
 & - \underbrace{0.5 \rho A_w R_d |v(t) - v_f(t)| (v(t) - v_f(t))}_{\theta_d(t)} \\
 & - \underbrace{F_n \left( \frac{\alpha_v |v(t)|}{F_n} + \alpha_d + (\alpha_s - \alpha_d) e^{-\left( \frac{|v(t)|}{v_s} \right)^2} \right) \text{sgn}(v(t))}_{\theta_f(t)} \\
 & \left. + \theta_m(t) \right]. \quad (2)
 \end{aligned}$$

The influence of wave radiation force is modeled as a LTI model,  $\dot{\boldsymbol{\sigma}}(t) = \mathbf{A}_r \boldsymbol{\sigma}(t) + \mathbf{B}_r v(t)$ , as thoroughly described in [2]. The coefficients  $S_s$ ,  $r_b$ , and  $m_{inf}$  represent the PTO mechanical spring stiffness, WEH's buoy radius, and hydrodynamic added mass, respectively. The parameters,  $\alpha_v$ ,  $\alpha_d$ , and  $\alpha_s$ , are the friction force coefficients, respectively. The dynamic model details can be found in [2].

The power take-off (PTO) system of the WEH consists of a three-phase permanent magnet linear generator (PMLG) along with a corresponding three-phase IGBT-based rectifier. The  $d$ - $q$  synchronous reference frame model of the PMLG can be

expressed as follows [11], [12]:

$$\frac{di_{sd}(t)}{dt} = -\frac{e_{sd}(t)}{L_s} - \frac{R_s}{L_s} i_{sd}(t) + \frac{\pi}{p_w} v(t) i_{sq}(t), \quad (3)$$

$$\frac{di_{sq}(t)}{dt} = -\frac{e_{sq}(t)}{L_s} - \frac{R_s}{L_s} i_{sq}(t) - \frac{\pi}{p_w} v(t) i_{sd}(t) - \frac{\pi \Psi_{PM}}{p_w} v(t), \quad (4)$$

where  $i_{sd}(t)$ ,  $i_{sq}(t)$ ,  $e_{sd}(t)$ , and  $e_{sq}(t)$  are the linear generator  $d$ - $q$  stator current and voltages components, respectively. The coefficients  $p_w$ ,  $R_s$ ,  $L_s$ , and  $\Psi_{PM}$  are the pole width, armature resistance, inductance, and flux linkage, respectively. The variable  $v(t)$  is the vertical velocity of the linear generator translator. A three-phase IGBT-based rectifier is employed to control the PMLG, which in turn controls the vertical motion of the WEH's buoy, as shown in Fig. 1. The rectifier stator voltage  $e_s(t)$  can be represented as a function of the switching signals  $\mathbf{S}(t)$  and DC-link voltage  $V_{dc}$  [13],

$$\begin{bmatrix} e_{sd}(t) \\ e_{sq}(t) \end{bmatrix} = \frac{V_{dc}(t)}{3} \mathbf{K}_{dq} \mathbf{K}_s \mathbf{S}(t). \quad (5)$$

where

$$\begin{aligned}
 \mathbf{K}_{dq} &= \sqrt{\frac{2}{3}} \begin{bmatrix} \cos\left(\frac{\pi}{p_w} x(t)\right) & -\sin\left(\frac{\pi}{p_w} x(t)\right) \\ \cos\left(\frac{\pi}{p_w} x(t) - \frac{2\pi}{3}\right) & -\sin\left(\frac{\pi}{p_w} x(t) - \frac{2\pi}{3}\right) \\ \cos\left(\frac{\pi}{p_w} x(t) + \frac{2\pi}{3}\right) & -\sin\left(\frac{\pi}{p_w} x(t) + \frac{2\pi}{3}\right) \end{bmatrix}^\top, \\
 \mathbf{K}_s &= \begin{bmatrix} 2 & -1 & -1 \\ -1 & 2 & -1 \\ -1 & -1 & 2 \end{bmatrix}, \mathbf{S}(t) = \begin{bmatrix} S_a(t) \\ S_b(t) \\ S_c(t) \end{bmatrix}
 \end{aligned}$$

Selecting the following state vector  $\mathbf{q}_k = [q_{1,k}, q_{2,k}, \mathbf{q}_{3,k}, q_{4,k}, q_{5,k}] = [x_k, v_k, \boldsymbol{\sigma}_k, i_{sd,k}, i_{sq,k}]$ , the input vector  $\mathbf{u}_k = [e_{sd,k}, e_{sq,k}]$ , and the output vector  $\mathbf{y}_k = \mathbf{q}_k$ . For the sampling time,  $T_s$ , the overall discrete model of the WEH system can be represented as follows:

$$\mathbf{q}_{k+1} = T_s \left[ \mathbf{A} \mathbf{q}_k + \mathbf{B} \mathbf{u}_k + \boldsymbol{\Xi}_k \right], \quad (6)$$

$$\mathbf{y}_k = \mathbf{C} \mathbf{q}_k, \quad (7)$$

where

$$\begin{aligned}
 \mathbf{q}_{k+1} &= \begin{bmatrix} q_{1,k+1} \\ q_{2,k+1} \\ \vdots \\ q_{5,k+1} \end{bmatrix}, \mathbf{q}_k = \begin{bmatrix} q_{1,k} \\ q_{2,k} \\ \vdots \\ q_{5,k} \end{bmatrix}, \\
 \mathbf{A} &= \begin{bmatrix} 0 & 1 & \mathbf{0}_{1 \times 4} & 0 & 0 \\ \frac{-S_s}{m+m_{inf}} & 0 & \frac{-\mathbf{C}_r}{m+m_{inf}} & 0 & \frac{-3\pi \Psi_{PM}}{2p_w(m+m_{inf})} \\ \mathbf{0}_{4 \times 1} & \mathbf{B}_r & \mathbf{A}_r & \mathbf{0}_{4 \times 1} & \mathbf{0}_{4 \times 1} \\ 0 & 0 & \mathbf{0}_{1 \times 4} & \frac{-R_s}{L_s} & 0 \\ 0 & \frac{-\pi \Psi_{PM}}{p_w} & \mathbf{0}_{1 \times 4} & 0 & \frac{-R_s}{L_s} \end{bmatrix}, \\
 \mathbf{B} &= \begin{bmatrix} 0 & 0 & \mathbf{0}_{1 \times 4} & -\frac{1}{L_s} & 0 \\ 0 & 0 & \mathbf{0}_{1 \times 4} & 0 & -\frac{1}{L_s} \end{bmatrix}^\top, \mathbf{C} = \begin{bmatrix} \mathbf{0}_{1 \times 6} & 1 & 0 \\ \mathbf{0}_{1 \times 6} & 0 & 1 \end{bmatrix}, \\
 \boldsymbol{\Xi}_k &= [\Xi_{1,k} \quad \Xi_{2,k} \quad \boldsymbol{\Xi}_{3,k} \quad \Xi_{4,k} \quad \Xi_{5,k}]^\top, \\
 \Xi_{1,k} &= 0, \Xi_{2,k} = -\frac{1}{m+m_{inf}} \left[ -\theta_{ex,k} \right]
 \end{aligned}$$

$$\begin{aligned}
& + \pi \rho g r_b^2 \left(1 - \frac{|q_{1,k}| |q_{1,k}|}{3r_b^2}\right) q_{1,k} - \frac{3\pi \Psi_{PM}}{2p_w} q_{5,k} \\
& + 0.5 \rho A_w R_d |q_{2,k} - v_{f,k}| (q_{2,k} - v_{f,k}) \\
& + F_n \alpha_d \tanh(\beta q_{2,k}) + \alpha_v q_{2,k} \\
& + F_n (\alpha_s - \alpha_d) e^{-\left(\frac{|q_{2,k}|}{v_s}\right)^2} \tanh(\beta q_{2,k}) \Big], \\
\Xi_{3,k} &= \mathbf{0}_{4 \times 1}, \Xi_{4,k} = \frac{\pi}{p_w} q_{2,k} q_{5,k}, \\
\Xi_{5,k} &= -\frac{\pi}{p_w} q_{2,k} q_{4,k}, \mathbf{U}_k = \frac{V_{dc,k}}{3} \mathbf{K}_{dq} \mathbf{K}_s \mathbf{S}_k.
\end{aligned}$$

### III. PROPOSED PREDICTIVE CONTROLLER DESIGN

The MPC approach being suggested eliminates the need for a predetermined reference signal. Instead, it relies on optimizing a cost function using an online search method called finite control set (FCS) to determine the optimal switching state of the machine-side rectifier in real-time. This is achieved by predicting the future states of the WEH system one sample ahead. All permissible switching permutations of rectifier are shown in Table 1. The switching states that maximizes the following objective function is selected to fire the rectifier switches,

$$\max_{\mathbf{U}_k} J_{k+1|k} = J_k + \left[ \frac{3T_s}{2} \tilde{\mathbf{y}}_{k+1|k} \mathbf{U}_k \right] W_k, \quad (8)$$

where  $J_k$  is the WEH converted energy at  $k$ . The prediction model is derived from the model stipulated in (6)-(7) as follows

$$\tilde{\mathbf{q}}_{k+1|k} = T_s \left[ \mathbf{A} \tilde{\mathbf{q}}_k + \mathbf{B} \mathbf{U}_k + \tilde{\Xi}_k \right], \quad (9)$$

$$\tilde{\mathbf{y}}_{k+1|k} = \mathbf{C} \tilde{\mathbf{q}}_{k+1|k}, \quad (10)$$

where the vectors  $\tilde{\mathbf{q}}_{k+1|k}$  and  $\tilde{\mathbf{y}}_{k+1|k}$  represent the predicted state and output vectors at  $k+1$ ,  $\tilde{\mathbf{q}}_k$  is the estimated state vector, and  $\mathbf{U}_k$  is the PTO control effort. To impose a soft constraint into the cost function,  $W_k$  is used to constrain the PMLG quadrature current component  $\tilde{q}_{5,k+1|k}$  and is expressed as follows

$$W_k = \begin{cases} 1 & \text{if } -I_s^* \leq \tilde{q}_{5,k+1|k} \leq I_s^* \\ 1 \times 10^{-6} & \text{otherwise} \end{cases} \quad (11)$$

where  $I_s^*$  represents the PMLG current limit. At each time instant  $k$ , it is only necessary to measure the PMLG three-phase stator currents of the using current transducers. The excitation force estimator is implemented similar to the method depicted in [2] is used to estimate the state vector  $\tilde{\mathbf{q}}_k$  along with the wave excitation force  $\theta_{e,k}$  using the three-phase stator current measurement as shown in Fig. 1.

### IV. REFERENCE-BASED CONTROL STRATEGY

For the sake of comparison, the performance of the proposed RLPC strategy is evaluated against the benchmark reference-based predictive control strategy denoted here as RBPC. The

TABLE I  
PTO RECTIFIER SWITCHING STATES

$S_a$	$S_b$	$S_c$	Voltage Vector $\mathbf{V}$
0	0	0	$\mathbf{V}_0 = \mathbf{0}$
1	0	0	$\mathbf{V}_1 = \frac{2}{3} V_{dc}$
1	1	0	$\mathbf{V}_2 = \frac{1}{3} V_{dc} + j \frac{\sqrt{3}}{3} V_{dc}$
0	1	0	$\mathbf{V}_3 = -\frac{1}{3} V_{dc} + j \frac{\sqrt{3}}{3} V_{dc}$
0	1	1	$\mathbf{V}_4 = -\frac{2}{3} V_{dc}$
0	0	1	$\mathbf{V}_5 = -\frac{1}{3} V_{dc} - j \frac{\sqrt{3}}{3} V_{dc}$
1	0	1	$\mathbf{V}_6 = \frac{1}{3} V_{dc} - j \frac{\sqrt{3}}{3} V_{dc}$
1	1	1	$\mathbf{V}_7 = \mathbf{0}$

TABLE II  
SIMULATION PARAMETERS

Parameter (symbol)	Value (Unit)
$T_s$	$1 \times 10^{-4}$ (s)
$m$	58000 (kg)
$\rho$	1025 (kg/m <sup>3</sup> )
$A_w$	28 (m <sup>2</sup> )
$m_{inf}$	28990 (kg)
$r_b$	3 (m)
$R_d$	1
$S_s$	42000 (N/m)
$F_n$	12300 (N)
$\alpha_d, \alpha_v, \alpha_s$	1, 2, 2
$v_s$	1 (m/s)
$\beta$	10
$V_{dc}$	690 (V)
$R_s$	1.4 ( $\Omega$ )
$L_s$	34 (mH)
$\Psi_{PM}$	19.8 (Wb)
$p_w$	45 (mm)

reference PTO electromagnetic force,  $\theta_{m,k}^*$  can be evaluated at every time instant  $k$  as

$$\theta_{m,k}^* = -|Z_i(\omega)| v_k, \quad (12)$$

where the WEH internal hydrodynamic impedance,  $Z_i(\omega)$ , and it is calculated as elaborated in [4].

### V. RESULTS AND DISCUSSION

To assess the efficacy of the implemented control strategies, simulations are conducted using MATLAB/Simulink using irregular sea environments. A comparative analysis is performed between the proposed RLPC strategy and the RBPC strategy. The simulation parameters are shown Table. II. Initially, an irregular sea state is employed to evaluate the mechanical and electrical performance of the wave energy harvester (WEH) operating under the RLPC strategy. The sea state consists of three irregular waves, each lasting 100 s, which are combined into a single 300 s wave for analysis. The wave train is a concatenated sea states with their characteristics ordered as follows:  $H_s = 2$  m and  $\omega_p = 0.48$  rad/s,  $H_s = 4.75$  m and  $\omega_p = 0.63$  rad/s, and  $H_s = 2.5$  m and  $\omega_p = 0.45$  rad/s. The resulting dynamics of the buoy motion, specifically the displacement and velocity, are depicted in Figure 2. The buoy displacements are as high as the wave elevation for wave portions with large peak periods (i.e.,  $\omega_p = 0.48$  rad/s and

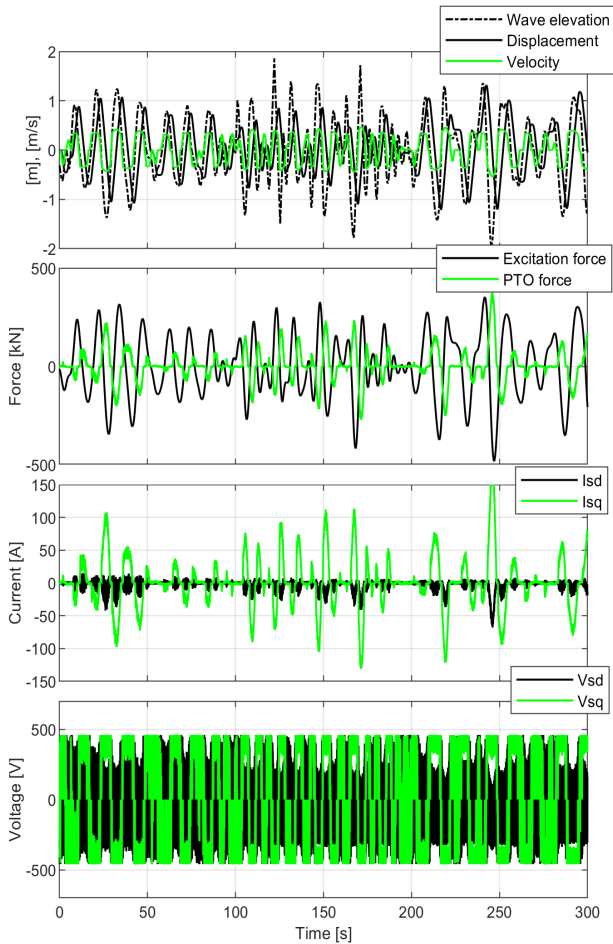


Fig. 2. WEH dynamics under the suggested control strategy for 300 s irregular sea environment.

$\omega_p = 0.45$  rad/s), whereas the velocity is stabilized at 0.5 m/s. The averaged linear generator force is approximately 47 kN, while its max-to-average ratio is 6.5. The shape and magnitude of the generator stator current  $q$  component is observed to be in agreement with the generator force signal. The controlled switching signal  $S(k)$ , is also shown. The instantaneous wave excitation power is shown in Fig. 3. The PTO absorbed power and converted power are both unidirectional, indicating the damping nature of the RLPC. The max-to-average ratio of the WEH is approximately 9.3. The absorbed power max-to-average ratio is almost 12, which is in agreement with the typical ratio values obtained when resistive loading technique is deployed. The system energy profiles are shown in Fig. 3. Subsequently, the cumulative electric energy is approximately 4.5 MJ, corresponding to an overall wave-to-wire conversion efficiency of 58 % and a PTO efficiency of approximately 82 %.

The evaluation of the RLPC strategy is conducted in comparison to the RBPC strategy, to determine its effectiveness. As depicted in Fig. 4, the two control strategies resulted

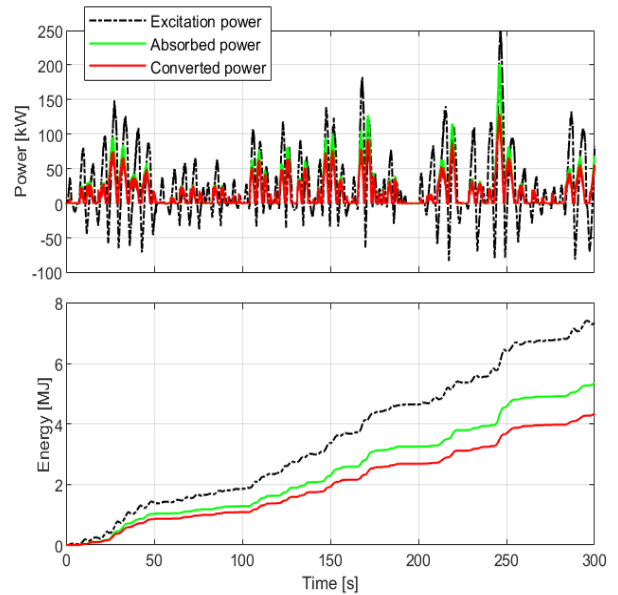


Fig. 3. Excitation, absorbed, and converted power and energy waveforms.

in different PTO force signals. The WEH under the RLPC needed approximately 47% lower control force compared with the RBPC. In regard to the converted power, Fig. 4 suggests that the energy is bidirectional for RBPC, which indicates that the active power moves reciprocally between the linear generator and the DC-link capacitor, unlike the case with RLPC. In Figure 4, the accumulated energy recorded at the output terminals of the linear generator is presented, demonstrating that the RLPC strategy surpasses the RBPC strategy by approximately 14%.

## VI. CONCLUSION

In this study, a novel estimator-based predictive control strategy is proposed for controlling point absorber wave energy harvesters (WEHs). The control strategy utilizes an online search technique to determine the optimal switching functions of the PTO's three-phase rectifier at each time step, eliminating the need for a pre-defined reference trajectory. The proposed RLPC control strategy demonstrates practical damping control, leading to a noticeable increase in energy conversion while utilizing less power take-off (PTO) resources. This efficient utilization of PTO resources allows for the adoption of PTO systems with lower power ratings, thus reducing overall system costs.

## REFERENCES

- [1] Yuhani, Wimalaratna, A. Hassan, Hadi, Afrouzi, K. Mehranzamir, J. Ahmed, B. Siddique, and S. Liew, "Comprehensive review on the feasibility of developing wave energy as a renewable energy resource in Australia", *Cleaner Energy Systems*, vol. 3, pp. 100021, 2022.
- [2] M. Jama, B. F. Mon, A. Wahyudie and S. Mekhilef, "Maximum Energy Capturing Approach for Heaving Wave Energy Converters Using an Estimator-Based Finite Control Set Model Predictive Control," *IEEE Access*, vol. 9, pp. 67648-67659, 2021.

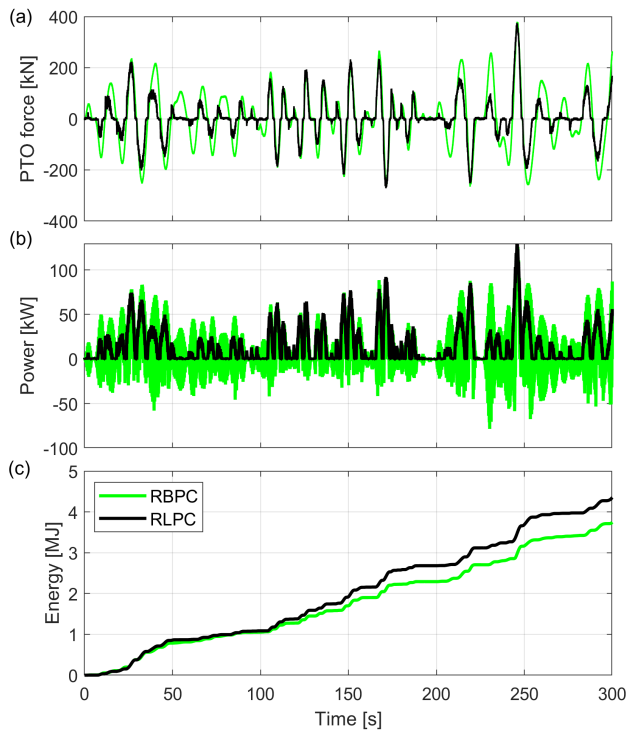


Fig. 4. Performances of RLPC and RBPC strategies

- [3] A. Wahyudie and M. Jama, "Perspectives on Damping Strategy for Heaving Wave Energy Converters", *IEEE Access*, vol. 5, pp. 22224-22233, 2017.
- [4] John. Ringwood, S. Zhan, and N. Faedo, "Empowering wave energy with control technology: Possibilities and pitfalls", *Annual Reviews in Control*, Vol. 55, pp. 18-44, 2023.
- [5] M. Jama, A. Wahyudie, and H. Noura, "Robust predictive control for heaving wave energy converters", *Control Engineering Practice*, vol. 77, pp. 138-149, 2018.
- [6] M. Jama, H. Noura, and A. Wahyudie, and A. Assi, "Enhancing the performance of heaving wave energy converters using model-free control approach," *Renewable Energy*, vol. 83, pp. 931-941, 2015.
- [7] A. Burgaç and H. Yavuz, "Fuzzy Logic based hybrid type control implementation of a heaving wave energy converter", *Energy*, vol. 170, pp. 1202-1214, 2019.
- [8] A. Shadmani, M. Nikoo, A. Gandomi, R. Wang, and B. Golparvar, "A review of machine learning and deep learning applications in wave energy forecasting and WEC optimization", *Energy Strategy Reviews*, vol. 49, pp.101180, 2023.
- [9] B. Mon et al., "Assessment of Damping Control Using Maximum Power Point Tracking Methods for Heaving Wave Energy Converters," *IEEE Access*, vol. 9, pp. 168907-168921, 2021.
- [10] E. Amon, T. Brekken, and A. Schacher, "Maximum power point tracking for ocean wave energy conversion," *IEEE Trans. Ind. Appl.*, vol. 48, pp. 1079-1086, 2012.
- [11] H .Said, D. García-Violini, and J. Ringwood, "Wave-to-grid (W2G) control of a wave energy converter", *Energy Conversion and Management: X*, Vol. 14, pp. 100190, 2022.
- [12] A. Wahyudie, T. Susilo, M. Jama, B. Mon and H. Shaaref, "Design of a double-sided permanent magnet linear generator for laboratory scale ocean wave energy converter," *OCEANS 2017 - Anchorage*, Anchorage, AK, USA, 2017, pp. 1-5.
- [13] P. Kou, D. Liang, J. Li, L. Gao, and Q. Ze, "Finite-Control-Set Model Predictive Control for DFIG Wind Turbines," *IEEE Transaction on Automation Science and Engineering*, vol. 15, pp. 1004-1013, 2018.